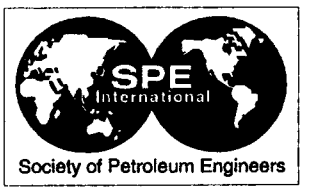

SPE 39802

Gel Treatments for Reducing Channeling in Naturally Fractured Reservoirs

R. S. Seright, SPE, and Robert Lee, SPE, New Mexico Institute of Mining and Technology

This paper was prepared for presentation at the 1998 SPE Permian Basin Oil and Gas Recovery Conference held in Midland, Texas, 25–27 March 1998.

Abstract

This paper considers some of the reservoir variables that affect the severity of channeling and the potential of gel treatments for reducing channeling through naturally fractured reservoirs. We performed extensive tracer and gel placement studies using two different simulators. We show that gel treatments have the greatest potential when the conductivities of fractures that are aligned with direct flow between an injector-producer pair are at least 10 times the conductivity of off-trend fractures. Gel treatments also have their greatest potential in reservoirs with moderate to large fracture spacing. Produced tracer concentrations from interwell tracer studies can help identify reservoirs that are predisposed to successful gel applications. Our simulation studies also show how tracer transit times can be used to estimate the conductivity of the most direct fracture. The effectiveness of gel treatments should be insensitive to fracture spacing for fractures that are aligned with the direct flow direction. The effectiveness of gel treatments increases with increased fracture spacing for fractures that are not aligned with the direct flow direction.

Introduction

Some of the most successful gel treatments have been applied to reduce channeling in naturally fractured reservoirs.[1-5] Therefore, a need exists to identify which characteristics of naturally fractured reservoirs indicate good candidates for gel applications. This paper considers some of the reservoir variables that affect the severity of channeling and the potential of gel treatments for reducing channeling through naturally fractured reservoirs.

Available Characterization Methods

At least three books describe reservoir engineering in naturally fractured reservoirs.[6-8] These books concentrate on oil and gas recovery during primary production. In contrast, this paper focuses on correcting channeling problems during secondary recovery operations.

Various logging methods have been used to detect and characterize fractures (Chapter 3 of Ref. 6, Chapter 2 of Ref. 7, and Chapter 5 of Ref. 8). Caution must be used with these methods since they usually measure properties at or very near the wellbore. The value of these methods can be increased if the wellbore is deviated to cross the different fracture systems (i.e., fractures with different orientations).

Pressure transient analyses have often been used to characterize fractured reservoirs (Chapter 4 of Ref. 6, Chapter 4 of Ref. 7, Chapters 6-8 of Ref. 8, and Ref. 9). Reportedly, these methods can estimate the fracture volume, the fracture permeability, and, possibly under some circumstances, the minimum spacing between fractures. Pressure interference tests can also indicate fracture orientation. In addition to unsteady-state methods, steady-state productivity indexes were also suggested as a means to estimate fracture permeability.

Interwell tracer studies provide valuable characterizations of fractured reservoirs, especially in judging the applicability of gel treatments to reduce channeling.[10-13] Interwell tracer data provides much better resolution of reservoir heterogeneities than pressure transient analysis.[14] Tracer results can indicate (1) whether fractures are present and if those fractures are the cause of a channeling problem, (2) the location and direction of fracture channels, (3) the fracture volume, (4) the fracture conductivity, and (5) the effectiveness of a remedial treatment (e.g., a gel treatment) in reducing channeling. Several models are available to analyze tracer results.[13-19]

In this paper, we present some simple concepts to assess the applicability of gel treatments in naturally fractured reservoirs—in particular, when channeling occurs between injector-producer pairs.

Representation of a Naturally Fractured Reservoir

When modeling naturally fractured reservoirs, the fracture systems generally have been envisioned as slabs (i.e., one set of parallel fractures), columns (i.e., two intersecting sets of parallel vertical fractures), or cubes (i.e., three intersecting sets of parallel fractures—two vertical and one horizontal). Geostatistics have also been used to describe fracture distributions. In this paper, we focus on the column model. For simplicity, assume that a naturally fractured reservoir consists of a regular pattern of north-south fractures intersected by east-

west fractures (see **Fig. 1**). For a given number, n, of fractures that are oriented in the north-south direction (the y-direction), 2n-1 fractures are oriented in the east-west direction (the x-direction). Fig. 1 illustrates a numbering scheme for the fractures (specifically for the case where n=11). For our base case, one injection well and one production well were located at either end of the central east-west fracture. Also, the distance between fractures was the same in both the x- and y-directions. (Later, we will consider wells where the producer is not on the central east-west fracture. Also, fracture spacing will be varied in different directions.) We assumed that flow through the rock is negligible compared with that through the fractures and that the system is incompressible. Furthermore, fractures in the y-direction are assumed to have a conductivity, $(k_f w_f)_y$, and fractures in the x-direction are assumed to have a different conductivity, $(k_f w_f)_x$. A conductivity ratio, R, is defined using Eq. 1.

$$R = (k_f w_f)_x / (k_f w_f)_y \quad \ldots\ldots (1)$$

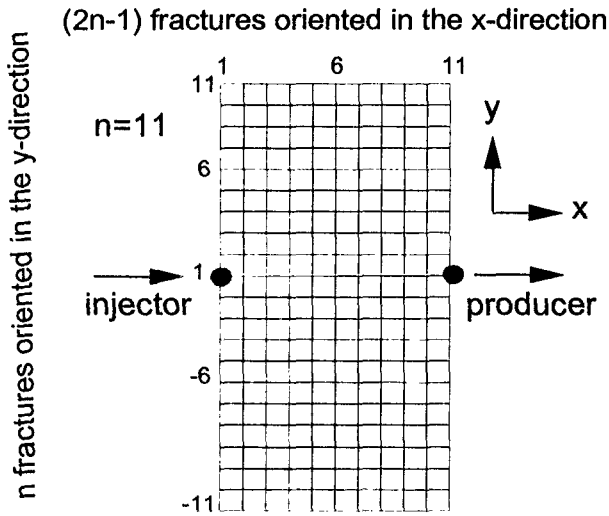

Fig. 1—Plan view of an injector-producer pair in a simple naturally fractured reservoir.

Ref. 20 describes two simulators (denoted C and E) that were used to determine pressures, flow rates, and front positions when a water tracer, a gelant, or a gel was injected into a fracture pattern. Simulator C assumed that gelant or tracer was injected continuously with a unit-mobility displacement without dispersion. In contrast, Simulator E was more sophisticated—allowing injection of banks of gelant, gel, or tracer and also accounting for dispersion of the banks. Simulator E was most useful for systems with relatively few fractures (i.e., with n-values of 21 or less). Simulator C was useful for obtaining relatively rapid results for systems with large numbers of fractures (i.e., with n-values up to 101).

Tracer Transit Times In a Single Fracture

During a unit-mobility displacement, the time required for a tracer to travel between an injector-producer pair often provides a useful characterization of a fractured reservoir.[10-13] Of course, the tracer transit time depends on a number of variables, including the pressure drop between the wells (Δp), the distance between wells (L), the number, orientation, and conductivity ($k_f w_f$) of the connecting fractures, and the viscosity of the fluid in the fractures (μ). We use the transit time associated with a single direct fracture as a means to normalize transit times for our fractured systems. If a reservoir contains only one fracture (with fracture height, h_f) that leads directly from the injector to the producer and flow through the rock matrix can be neglected, the Darcy equation determines the volumetric flow rate (q).

$$q = \Delta p\, k_f w_f h_f / (L\mu) \quad \ldots\ldots (2)$$

The transit time (t) for a tracer is estimated from the fracture volume ($h_f w_f L \phi_f$) divided by q.

$$t = h_f w_f L \phi_f / q = w_f L^2 \mu \phi_f / [\Delta p\, (k_f w_f)] \quad \ldots\ldots (3)$$

Given the fracture conductivity, the effective average fracture width, w_f, can be estimated using Eq. 4 if w_f is expressed in feet and $k_f w_f$ is expressed in darcy-feet.[21]

$$w_f = 5.03 \times 10^{-4} (k_f w_f)^{1/3} \quad \ldots\ldots (4)$$

Fig. 2 plots expected tracer transit times from Eq. 3 versus fracture conductivity and pressure drop when L=1,000 ft, μ=1 cp, and ϕ_f=1. As an example, for a pressure drop of 80 psi, Fig. 2 predicts a transit time of one day for a 1,000-ft-long fracture with a conductivity of 1 darcy-feet.

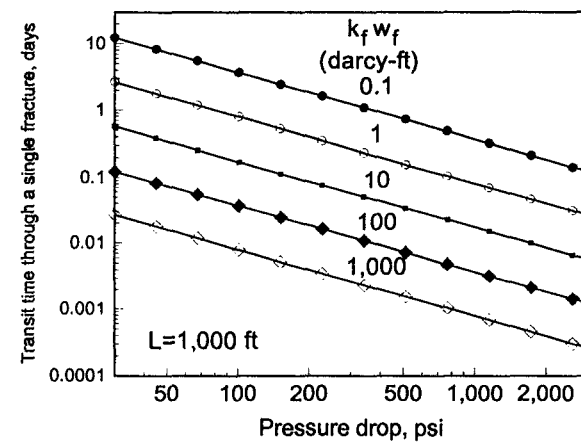

Fig. 2—Transit times through a single 1,000-ft-long fracture.

Although the above analysis provides a simple and useful means to roughly estimate tracer transit times, one should recognize that dispersion affects the profile of produced tracer concentrations versus time or volume throughput. For example, **Fig. 3** (from Ref. 13) shows field results from two interwell tracer tests that were performed before and after application of a gel treatment in a limestone reservoir. For both tests, a slug of radioactive tracer was injected over a short time period, but the tracer was produced over the course of 140 days. In both cases, the first tracer was produced only four days after tracer injection into a well that was 450 feet from the producer. The peak

concentration was observed after 10 days for the tracer study before the gel treatment and after 37 days for the study after the gel treatment.

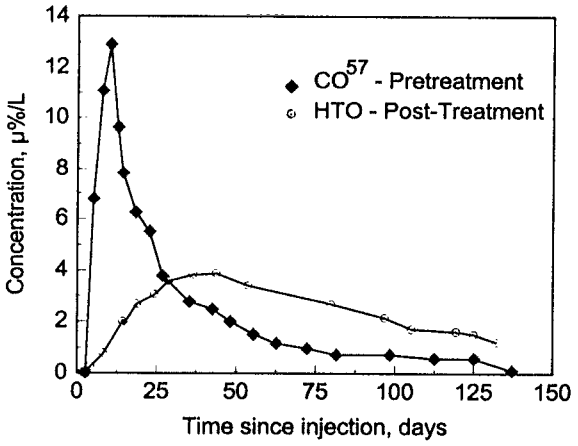

Fig. 3—Interwell tracer results before and after a gel treatment (after Ref. 13). Injection: 250 BWPD. Production: 550 BWPD.

Using tracer results, Tester *et al.*[11] considered several methods to estimate the volume associated with a fracture channel. They suggested that the best estimate of the volume of a fracture path is provided by the modal volume. This volume is associated with the peak concentration in the produced tracer distribution. For example, in Fig. 3, the peak concentration during a tracer study before the gel treatment was noted about 10 days after tracer injection. Based on other information provided in Ref. 13, about 20% of the production rate of 550 BWPD was attributed to the well where tracer was injected. Thus, the estimated volume of the dominant fracture path was 0.2 x 550 x 10 or 1,100 bbls.

Tester *et al.*[11] noted that other volume measures could be determined from the tracer curves, including integral mean volumes and median volumes. However, they observed that these volumes are weighted to overestimate the fracture volume in most circumstances.

If dispersion during flow through a single fracture (with no leakoff) was caused only by laminar mixing, a tracer would first arrive at the end of a fracture after injecting two-thirds of one fracture volume.[22,23] In the examples shown in Fig. 3, tracer breakthrough occurred at 40% and 11% of the volumes and times associated with the peak concentrations. These results suggest that considerable dispersion occurred in the field examples. Also, the tracer front should completely pass after injection of a few fracture volumes (i.e., a few thousand barrels). Instead the tracer profile was dispersed over 140 days (≈ 70 fracture volumes). This dispersion reflects the range of pathways from the injection well to the production well.[11,13] Early tracer production reflects the most rapid pathways, while late tracer production indicates long or circuitous pathways, dead ends, or possibly chemical exchange in the reservoir.[11,13] As will be evident in the next section, a wide range of pathways are available in naturally fractured reservoirs.

Transit Times In a Fracture System

Simulator C was used to determine times required for a tracer to travel from an injection well to a production well in a naturally fractured system. These calculated transit times reflect the most rapid pathways between the wells. In all cases, the "reservoir" looked like Fig. 1. Also, a unit-mobility displacement was used, and a fixed pressure drop was applied between the wells. The transit times from this program were normalized by dividing by the time calculated using Eq. 3. These dimensionless transit times are plotted in **Fig. 4**. In this figure, the fracture conductivity ratios, R, ranged from 0.001 to 1,000. The number of fractures oriented in the y-direction, n, ranged from 3 to 101.

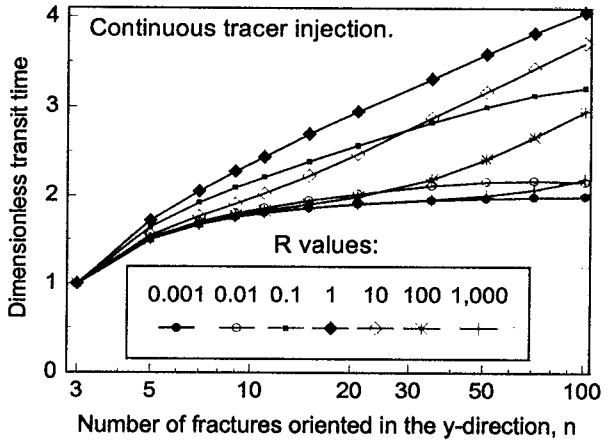

Fig. 4—Injector-producer tracer transit times in naturally fractured systems relative to that for a single direct fracture (unit-mobility displacement, fixed pressure drop, continuous injection, no dispersion). (Simulator C.)

Simulator E was used to confirm the results shown in Fig. 4. Similar conditions were applied for both sets of simulations. Details of these simulations can be found in Ref. 20. As mentioned earlier, Simulator E considered injection of a tracer bank that can experience dispersion, while the Simulator C only considered continuous tracer injection with no dispersion. For runs made with Simulator E, the volume of the injected tracer bank was 10% of the total fracture volume of the system.

For the range of conditions examined, Fig. 4 suggests that the transit time is not greatly sensitive to the R- or n-values. In particular, we see, at most, a four-fold variation in dimensionless transit times. These results indicate that tracer transit times will not help much in determining R- or n-values in field applications. With increasing n-values, the greatest variations occur when R=1 (fractures in the x-direction have the same conductivity as those in the y-direction). The smallest variations occur when R is very large or when R is near zero. Incidentally, under our conditions, the dimensionless transit time is unity when $n \leq 3$.

The fact that tracer transit times are not sensitive to R- or n-values suggests that transit times can be very useful when estimating the permeability or conductivity of the most direct fracture. To explain, Fig. 4 indicates that the tracer transit time in a naturally fractured reservoir is usually between one and four

times the value for a single direct fracture (if n ≤ 101). Therefore, if the tracer transit time is measured, that value can be used in Eq. 5 (obtained by rearranging Eq. 3) to estimate the effective fracture permeability (within a factor of four).

$$k_f = L^2 \mu \phi_f / (t\, \Delta p) \quad \ldots\ldots (5)$$

If k_f is known in darcy units, Eq. 6 (obtained by rearranging Eq. 4) can be used to convert fracture permeability to fracture conductivity (in darcy-feet).

$$k_f w_f = 1.13 \times 10^{-5} (k_f)^{1.5} \quad \ldots\ldots (6)$$

Sweep Efficiency

The sweep efficiency in our model systems can be assessed by comparing flow rates through specific fractures. For example, an effective method to judge the severity of channeling is to compare the flow rate in the most direct fracture with the total injection rate. This comparison is made in **Fig. 5** for R-values ranging from 0.001 to 1,000 and for n-values ranging from 2 to 101. The y-axis in Fig. 5 shows the flow rate in the most direct x-direction fracture (i.e., the central east-west fracture in Fig. 1) divided by the total injection rate. More specifically, the flow rate in the most direct fracture was determined at the midpoint between the two wells.

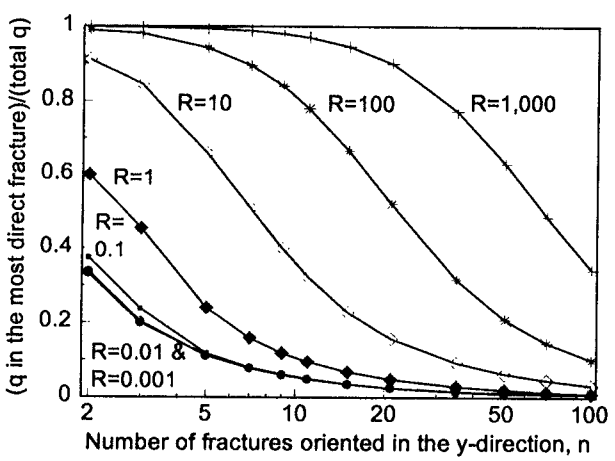

Fig. 5—Severity of channeling through the most direct x-direction fracture. (Simulator C.)

As expected, Fig. 5 shows that the most severe channeling occurs with the largest R-values (i.e., when fracture conductivity in the x-direction is much greater than that in the y-direction). When the R-values are 0.1 or less, the fraction of flow in the most direct fracture is low and nearly independent of the R-value—indicating that sweep efficiency is quite good. Fig. 5 suggests that channeling is generally not severe unless the R-value is 10 or greater.

Fig. 5 also indicates that the severity of channeling through the most direct fracture decreases with increased n-value. Recall from Fig. 1 that n is the number of fractures oriented in the y-direction, while 2n-1 fractures are oriented in the x-direction. In all figures in this paper, the distance between the two wells is fixed. So, as the n-value increases, the distance between fractures decreases. For example, if n=11, the distance between fractures will be 10 times greater than that when n=101.

Fig. 5 suggests a method to make interwell tracer studies useful when assessing the R- and n-values in field applications. When R is large and n is low to intermediate, the production rate is dominated by flow through the most direct fracture. Thus, if a tracer is injected continuously, the tracer concentration in the production well should stabilize at a high value under these conditions. Fig. 5 suggests that if the produced tracer concentration was 90% of the injected value, the R-value must be at least 10. However, this suggestion assumes that our production well is fed only by the fracture system to the left of the producer in Fig. 1. In a naturally fractured system, we expect a similar fluid supply from a fracture pattern to the right of the producer in Fig. 1. Thus, the expected tracer concentrations would be half of the values suggested by Fig. 5. Then, in the example above, if the produced tracer concentration was 45% of the injected value, the R-value must be at least 10.

Similar reasoning suggests that a produced tracer concentration of 30% indicates that the R-value is at least 1 and is probably at least 10 (from Fig. 5). Actually, this value is conservative. As mentioned earlier, dispersion during laminar flow in a single fracture is expected to result in a 33% dilution.[22,23] Therefore, a produced tracer concentration of 20% (i.e., 30% x 0.67) generally indicates an R-value of at least 10.

As will be shown shortly, gel treatments in naturally fractured reservoirs have the greatest potential when R-values are high and n-values are low to intermediate. In searching for a guideline to distinguish when a reservoir meets these conditions, a potentially useful indicator is a peak produced tracer concentration of at least 20% of the injected value. Of course, the potential for a gel treatment becomes greater as the peak produced tracer concentration increases above 20% of the injected value. When produced tracer concentrations are low, gel treatments are unlikely to be effective.

The above recommendation assumes that a sufficient tracer bank is injected. If the tracer bank is too small, dispersion will reduce the produced concentrations well below those suggested here. Of course, retention or degradation of the tracer can also have this effect. Thus, the tracer study must be designed properly in order for our recommendation to be of value.

When R ≤ 0.1, we found that the flow rate is basically the same through all x-direction fractures, regardless of the n-value.[20] The sweep efficiency is very high when the conductivity of the x-direction fractures is much less than that of the y-direction fractures. Obviously, no gel treatment is needed in this type of reservoir, since no significant channeling exists.

In contrast, when R ≥ 10, our simulations indicated that virtually no flow occurs through most of the x-direction fractures.[20] In these cases, most flow occurs through the most direct fracture or through fractures close to the most direct fracture.[20] Of course, these are the conditions where a gel treatment is expected to work best.

When R=1 (all fractures have the same conductivity), our studies revealed that the flow rate in the least direct fracture is about 20% of that in the most direct fracture.[20] Thus, the sweep

efficiency is still reasonably good, and we suspect that a gel treatment may not provide much benefit.

Fig. 5 was generated using Simulator C. As a check for these results, simulations were also performed using Simulator E. This program calculated the tracer concentrations that were produced after injecting a tracer bank equivalent to 10% of the total fracture volume.

Fig. 6 was generated using Simulator E. This figure plots the produced tracer concentration when n=11 for R-values ranging from 0.001 to 1,000. In agreement with the previous results and conclusions, Fig. 6 demonstrates that (1) the tracer transit time (as determined by tracer breakthrough) was not sensitive to R-value, (2) produced tracer concentrations were low (less than 10% of the injected values) when $R \leq 1$, and (3) peak produced tracer concentrations were relatively high when $R \geq 10$. These conclusions were supported by results using both simulators.[20]

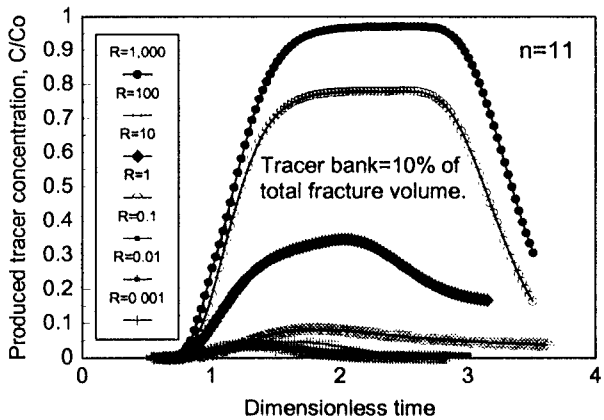

Fig. 6—Produced tracer concentrations when injecting a tracer bank with n=11. (Simulator E.)

Effect of Plugging the Most Direct Fracture

Ideally, a gel treatment should plug the most direct fracture without entering or damaging the secondary fractures. If this gel placement could be achieved, how would sweep efficiency be affected? More specifically, how rapidly would a water tracer travel between an injector and a producer after versus before a gel treatment? This question is addressed in **Fig. 7** for R-values ranging from 1 to 1,000 and for n-values ranging from 3 to 101. (Fig. 7 was generated using Simulator C.) The y-axis plots the ratio of breakthrough times—i.e., the transit time for a tracer after the most direct fracture was plugged divided by the tracer transit time before the most direct fracture was plugged.

Fig. 7 indicates that gel treatments have the greatest potential for reservoirs with high R-values and low to intermediate n-values. Gel treatments are not expected to provide much sweep improvement when $R \leq 1$.

Diagonally Oriented Fractures

We have focused on fractured systems where one central x-direction fracture directly connects the injector-producer pair. How would our results be affected if the fractures were oriented diagonally relative to the wells (i.e., at position 11,11 in Fig. 1)? In Ref. 20, we demonstrate that diagonally oriented fractures act like direct-fracture systems with low R-values. Careful consideration reveals that diagonally oriented fractures should provide acceptable sweep efficiencies, and they are poor candidates for gel treatments.

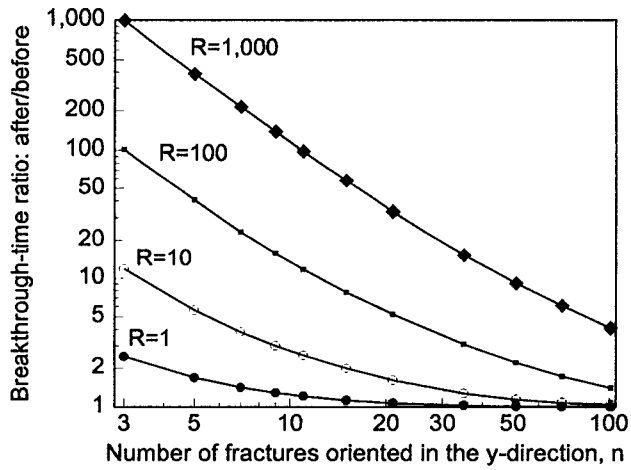

Fig. 7—Effect of plugging the most direct fracture. (Simulator C.)

Fig. 8 shows the effects of injecting a 0.1 fracture-volume tracer bank when n=11 and the producer was slightly off the direct east-west path. In this case, the injection well was located on the central x-direction fracture, and the production well was located one fracture north of the central x-direction fracture. In other words, in Fig. 8, the production well was located at coordinates (11,2), while the injection well was located at (1,1). Fig. 8 plots the relative produced tracer concentration (C/C_o) versus dimensionless time for R-values ranging from 1 to 1,000. The denominator used to determine the dimensionless time was the same for all four curves. Specifically, the denominator was the same transit time used when determining dimensionless times for Figs. 4 and 6.

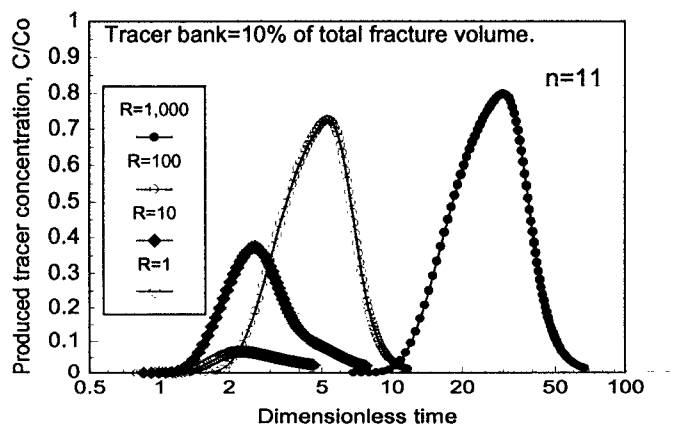

Fig. 8—Tracer curves when injector and producer were located at (1,1) and (11,2), respectively. (Simulator E.)

For cases where the injector-producer pairs were located at opposite ends of the central x-direction fracture, Fig. 6 shows that breakthrough times all occurred at dimensionless times around 0.8 and the peak-concentration times occurred at dimensionless times roughly around 2, regardless of the R-value. In contrast, when the producer was located one fracture off center, at (11,2), Fig. 8 shows that the breakthrough times and peak-concentration times increased with increased R-value. (The conductivities of x-direction fractures were fixed in this study.)

The behavior in Fig. 6 can be readily understood by remembering that in all cases, the central x-direction fracture had the same conductivity. Also, all injector-producer pairs represented in Fig. 6 were effectively separated by the same distance and experienced the same pressure drop. Therefore, we expected the interwell tracer transit time to be fairly insensitive to R-value. Recall that the results in Fig. 4 were consistent with this idea. As mentioned earlier, the tracer transit times provide an excellent means to estimate the permeability and conductivity of the most direct fracture (i.e., using Eqs. 5 and 6).

The behavior in Fig. 8 can be understood by recognizing that the most direct injector-producer pathways were slightly longer (specifically, 10% longer) than those associated with Fig. 6. Depending on the R-value, the resistance to flow added by the additional 10% of fracture pathway could significantly increase the transit time.

Interestingly, the tracer curves in Fig. 8 appear more peaked than those in Fig. 6, but the peak concentration values are fairly similar for the two figures. The R=1,000 case appears to be a slight exception, with the peak value in Fig. 8 being about 16% lower than that in Fig. 6. Simulations using larger tracer banks revealed that this was a dispersion effect—the peak values for the R=1,000 cases would have been much closer if a 0.5-fracture-volume tracer bank had been injected.[20]

Uneven Fracture Spacing

In the work described so far, the distance between adjacent x-direction fractures was the same as that for y-direction fractures. How would our results change if fracture spacing was different in the x- and y-directions? This question is addressed in **Figs. 9 and 10**. (Both figures were generated using Simulator C.) In Fig. 9, the reservoir contained 11 fractures oriented in the y-direction. The number of fractures oriented in the x-direction varied from 11 to 321. As a reminder, the case with 11 y-direction fractures and 21 x-direction fractures has the same fracture spacing in both directions (see Fig. 1). Also recall that the dimensions of the reservoir are fixed, so we simply change the fracture spacing or intensity when the number of fractures are varied. The case with 321 x-direction fractures has 16 times greater distance between y-direction fractures than between x-direction fractures.

Figs. 9 and 10 show the effect of fracture-spacing anisotropy on the breakthrough-time ratio. In both figures, the y-axis plots the tracer transit time after an ideal gel treatment divided by that before the gel treatment. The gel treatment was ideal because we assumed that the gel plugged the most direct fracture without damaging secondary fracture pathways. In Fig. 9, where the number of y-direction fractures was fixed at 11, note that the breakthrough-time ratio was remarkably insensitive to the number of fractures oriented in the x-direction.

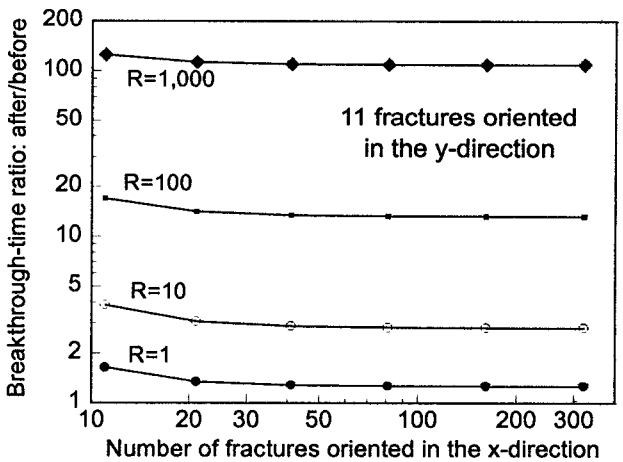

Fig. 9—Effect of plugging the most direct fracture when spacing for y-direction fractures is greater than for x-direction fractures.

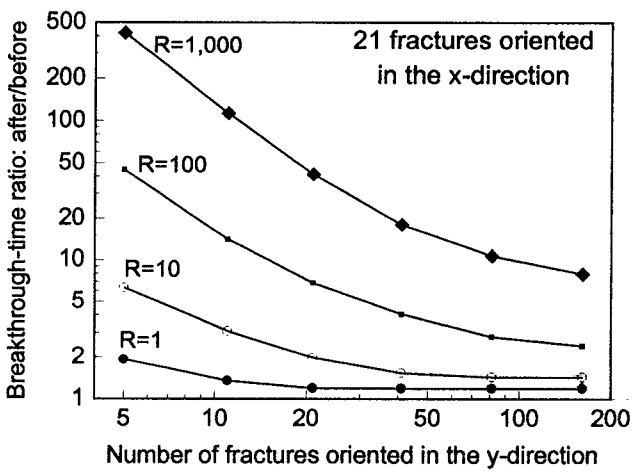

Fig. 10—Effect of plugging the most direct fracture when spacing for x-direction fractures is greater than for y-direction fractures.

In contrast, in Fig. 10, the number of x-direction fractures was fixed at 21, while the y-direction fractures varied from 5 to 161. The breakthrough-time ratio was sensitive to y-direction fracture spacing, especially for high R-values. The trends in Fig. 10 were similar to those in Fig. 7. This similarity suggests that variation in the spacing of y-direction fractures was responsible for the sensitivity to n-values seen in Fig. 7. Both Figs. 9 and 10 confirm that gel treatments have their greatest potential in reservoirs with high R-values (i.e., $R \geq 10$).

Gel Front Profiles

In previous work,[21] we showed that gels exhibit a pronounced shear-thinning behavior during extrusion through fractures. For a commonly used Cr(III)-acetate-HPAM gel, the gel resistance factor (F_r) was related to extrusion flux (u) using Eq. 7.

$$F_r = 2 \times 10^6 u^{-0.83} \text{ if } u \le 600 \text{ ft/d}$$
$$F_r = 10{,}000 \text{ if } 600 < u < 6{,}200 \text{ ft/d} \quad (7)$$
$$F_r = 4 \times 10^7 u^{-0.95} \text{ if } u \ge 6{,}200 \text{ ft/d}$$

Eq. 7 was incorporated into Simulator E, which we used to determine positions of gel fronts in naturally fractured systems. In these simulations, the injection and production wells were located at opposite ends of the central x-direction fracture in Fig. 1. Front profiles were determined when gel first arrived at the production well. The pressure drop and distance between wells were fixed at 735 psi and 1,312 ft, respectively. The conductivity of the x-direction fractures were fixed at 328 darcy-feet. (Thus, when R-values varied, the conductivity of the y-direction fractures was changed.) These specifications are needed because the simulations were performed with non-Newtonian gels. They were not needed for earlier simulations where Newtonian fluids were involved.

Fig. 11 shows gel front profiles when n=11 and R-values ranged from 1 to 1,000. The axes in this figure were normalized to extend from the injector to the producer (for the x-axis) and from the injector to the top (north) reservoir boundary (for the y-axis). Especially for R-values from 10 to 1,000, the distance of gel penetration in the y-direction fractures was fairly independent of the x-position, until the x-position approached unity (i.e., the vicinity of the production well).

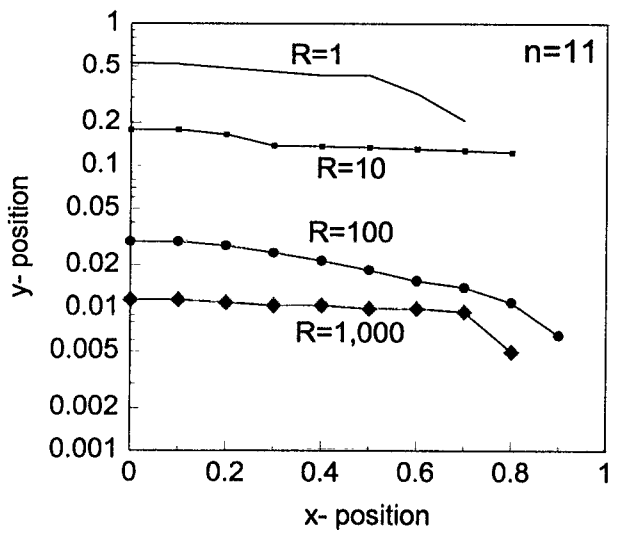

Fig. 11—Distances of gel penetration in the y-direction fractures when gel reaches the production well (Simulator E).

We performed additional simulations using R-values from 1 to 1,000 and n-values from 5 to 21. Half of the simulations involved gel injection (i.e., the rheology indicated by Eq. 7). The other half involved injection of gelants with a water-like viscosity. In general, the gels gave flatter front profiles (i.e., like Fig. 11) than those for the water-like gelants. However, for a given set of R- and n-values, the maximum distance of gel penetration into y-direction fractures was roughly the same as that for a water-like gelant. (This conclusion assumed that gravity and imbibition were negligible.)

For the case where n=11 and R=10, Fig. 11 suggests that gel will plug the three central x-direction fractures in Fig. 1 (because the gel penetrates between 10% and 20% of the distance in the y-direction). When R ≥ 100, Fig. 11 suggests that the gel will only plug the central x-direction fracture. Of course, for a given R-value, as the n-value increases (i.e., higher fracture intensity), the gel will plug a greater number of central x-direction fractures.

The objective of a gel treatment in a naturally fractured reservoir is to reduce or prevent flow through the most conductive, most direct fracture(s) without damaging the secondary fracture pathways. The secondary fractures are needed to allow injected water to displace oil and to allow oil to flow unimpeded to the production well.

To obtain the results shown in Fig. 11, we assumed that gel propagation was only affected by rheological effects (Eq. 7) during the extrusion process. However, gels can dehydrate or concentrate during extrusion if the fractures are sufficiently narrow.[25] In fractures with widths less than 0.04 inches, gel dehydration can retard gel propagation by factors up to 40. Since this dehydration becomes more pronounced as fracture conductivity and width decrease,[25] gel penetration into secondary fracture pathways could be much lower than otherwise expected.

Gels also require a minimum pressure gradient (i.e., a yield stress) in order to enter a fracture with a given conductivity.[25] This property could also help to optimize gel placement in naturally fractured reservoirs. For moderate to large fracture spacing and relatively high R-values, gel placement may approach the ideal case where only the central x-direction fracture is plugged by gel. In that case, Fig. 7 can be used to estimate the effectiveness of a gel treatment for a given set of R- and n-values.

In our future work, we hope to develop a methodology for sizing gel treatments in naturally fractured reservoirs.

Conclusions

In a naturally fractured reservoir, we define an R-value as the conductivity of fractures that are aligned with direct flow between an injector-producer pair divided by the conductivity of fractures that are not aligned with direct flow between wells. We also define an n-value as the number of fractures between an injector-producer pair, where these fractures are not aligned with the direct flow direction.

1. Gel treatments in naturally fractured reservoirs have the greatest potential when R-values are high (greater than 10).
2. Produced tracer concentrations from interwell tracer studies can be useful in identifying reservoirs with high R-values.
3. We propose that the potential for a gel treatment becomes greater as the peak produced tracer concentration increases above 20% of the injected value (for a properly designed tracer study). When produced tracer concentrations are low, gel treatments are unlikely to be effective.
4. Because tracer transit times are not sensitive to R- or n-values, they can be very useful when estimating the permeability or conductivity of the most direct fracture.

5. The effectiveness of gel treatments should be insensitive to fracture spacing for fractures that are aligned with the direct flow direction.
6. The effectiveness of gel treatments increases with increased fracture spacing for fractures that are not aligned with the direct flow direction.

Nomenclature

C = produced tracer concentration, g/m^3
C_o = injected tracer concentration, g/m^3
F_r = resistance factor (brine mobility before gel placement divided by gel mobility)
h_f = fracture height, ft [m]
k_f = fracture permeability, darcys [μm^2]
L = distance between wells, ft [m]
n = number of fractures oriented in the y-direction
Δp = pressure drop, psi [Pa]
q = flow rate, B/D [m^3/s]
R = fracture conductivity ratio defined by Eq. 1
t = time, days [s]
u = flux, ft/d [m/s]
w_f = fracture width, ft [m]
x = abscissa
y = ordinate
μ = viscosity, cp [mPa-s]
ϕ_f = effective porosity in a fracture

Acknowledgments

Financial support for this work is gratefully acknowledged from the United States Department of Energy (NPTO), BDM-Oklahoma, ARCO, British Petroleum, Chevron, Chinese Petroleum Corp., Conoco, Eniricerche, Exxon, Halliburton, Marathon, Norsk Hydro, Phillips Petroleum, Saga, Schlumberger-Dowell, Shell, Statoil, Texaco, and Unocal.

References

1. Sydansk, R.D. and Moore, P.E.: "Gel Conformance Treatments Increase Oil Production in Wyoming," *Oil & Gas J.* (Jan. 20, 1992) 40-45.
2. Moffitt, P.D.: "Long-Term Production Results of Polymer Treatments in Production Wells in Western Kansas," *JPT* (April 1993) 356-62.
3. Borling, D.C.: "Injection Conformance Control Case Histories Using Gels at the Wertz Field CO_2 Teriary Flood in Wyoming, USA," paper SPE 27825 presented at the 1994 SPE/DOE Symposium on Improved Oil Recovery, April 17-20.
4. Fullbright, G.D. *et al.*: "Evolution of Conformance Improvement Efforts in a Major CO_2 WAG Injection Project," paper SPE/DOE 35361 presented at the 1996 SPE/DOE Symposium on Improved Oil Recovery, Tulsa, April 21-24.
5. Tweidt, L.I. *et al.*: "Improving Sweep Efficiency in the Norman Wells Naturally Fractured Reservoir Through the Use of Polymer Gels: A Field Case History," paper SPE 38901 presented at the 1997 SPE Annual Technical Conference and Exhibition, San Antonio, Oct. 5-8.
6. Aguilar, R.: *Naturally Fractured Reservoirs*, Pennwell, Tulsa, OK (1980).
7. Saidi, A.M.: *Reservoir Engineering of Fractured Reservoirs*, General Printing, Singapore (1987).
8. Van Golf-Racht, T.D.: *Fundamentals of Fractured Reservoir Engineering*, Elsevier Scientific Publishing, Amsterdam (1982).
9. Gilman, J.R, Hinchman, S.B., and Svaldi, M.A.: "Using Polymer Injectivity Tests to Estimate Fracture Porosity in Naturally Fractured Reservoirs," paper SPE 25880 presented at the 1993 Rocky Mountain Regional/Low Permeability Reservoirs Symposium, Denver, April 12-14.
10. Wagner, O.R.: "The Use of Tracers in Diagnosing Interwell Reservoir Heterogeneities—Field Results," *JPT* (Nov. 1977) 1410-1416.
11. Tester, J.W., Bivins, R.L., and Potter, R.M.: "Interwell Tracer Analyses of a Hydraulically Fractured Granitic Geothermal Reservoir," *SPEJ* (Aug. 1982) 537-554.
12. Beier, R.A. and Sheely, C.Q.: "Tracer Surveys to Identify Channels for Remedial Work Prior to CO_2 Injection at MCA Unit, New Mexico," paper SPE 17371 presented at the 1988 SPE/DOE Enhanced Oil Recovery Symposium, Tulsa, April 17-20.
13. Lichtenberger, G.J.: "Field Applications of Interwell Tracers for Reservoir Characterization of Enhanced Oil Recovery Pilot Areas," paper SPE 21652 presented at the 1991 SPE Production Operations Symposium, Oklahoma City, April 7-9.
14. Datta-Gupta, A. Vasco, D.W., and Long, J.C.S.: "Sensitivity and Spacial Resolution of Transient Pressure and Tracer Data for Heterogeneity Characterization," paper SPE 30589 presented at the 1995 SPE Annual Technical Conference and Exhibition, Dallas, Oct. 22-25.
15. Hagoort, J.: "The Response of Interwell Tracer Tests in Watered-Out Reservoirs," paper SPE 11131 presented at the 1982 SPE Annual Technical Conference and Exhibition, New Orleans, Sept. 26-29.
16. Agca, C., Pope, G.A., and Sepehrnoori, K.: "Modelling and Analysis of Tracer Flow in Oil Reservoirs," *J. Petroleum Science and Engineering*, 4 (1990) 3-19.
17. Shinta, A.A. and Kazemi, H.: "Tracer Transport in Characterization of Dual-Porosity Reservoirs," paper SPE 26636 presented at the 1993 SPE Annual Technical Conference and Exhibition, Houston, Oct. 3-6.
18. Datta-Gupta, A. *et al.*: "Detailed Characterization of a Fractured Limestone Formation by Use of Stochastic Inverse Approaches," *SPEFE* (Sept. 1995) 133-140.
19. Jetzabeth, R. *et al.*: "Tracer-Test Interpretation in Naturally Fractured Reservoirs," *SPEFE* (Sept. 1995) 186-192.
20. Seright, R.S.: "Improved Methods for Water Shutoff," Annual Technical Progress Report (U.S. DOE Report DOE/PC/91008-4), U.S. DOE Contract DE-AC22-94PC91008, BDM-Oklahoma Subcontract G4S60330 (Nov. 1997) 50-75, 156-222.
21. Seright, R.S.: "Use of Preformed Gels for Conformance Control in Fractured Systems," *SPEPF* (Feb. 1997) 59-65.
22. Perkins, T.K. and Johnston, O.C.: "A Review of Diffusion and Dispersion in Porous Media," *SPEJ* (March 1963) 70-84.
23. Bird, R.B., Stewart, W.E., and Lightfoot, E.N.: *Transport Phenomena*, John Wiley & Sons, New York (1960) 11, 42-63.
24. Seright, R.S.: "Gel Placement in Fractured Systems," *SPEPF* (Nov. 1995) 241-248.
25. Seright, R.S.: "Gel Dehydration During Extrusion Through Fractures," paper SPE 39957 presented at the 1998 SPE Rocky Mountain Regional/Low-Permeability Reservoirs Symposium and Exhibition held in Denver, April 5-8.